CellPress

Multifaceted Regulation of Somatic Cell Reprogramming by mRNA Translational Control

Soroush Tahmasebi,[1,2] Tommy Alain,[8] Vinagolu K. Rajasekhar,[3] Jiang-Ping Zhang,[1,4] Masha Prager-Khoutorsky,[5] Arkady Khoutorsky,[1,2] Yildirim Dogan,[6] Christos G. Gkogkas,[9] Emmanuel Petroulakis,[1,2] Annie Sylvestre,[1,2] Mohammad Ghorbani,[1,4] Sarah Assadian,[1,2] Yojiro Yamanaka,[1,7] Julia R. Vinagolu-Baur,[6] Jose G. Teodoro,[1,2] Kitai Kim,[6] Xiang-Jiao Yang,[1,2,4,*] and Nahum Sonenberg[1,2,4,*]

[1]The Rosalind and Morris Goodman Cancer Research Center, McGill University, Montréal, QC H3A 1A3, Canada
[2]Department of Biochemistry, McGill University, Montréal, QC H3A 1A3, Canada
[3]Department of Medicine, Memorial Sloan-Kettering Cancer Center, New York, NY 10065, USA
[4]Department of Medicine, McGill University Health Center, Montréal, QC H3A 1A3, Canada
[5]Centre for Research in Neuroscience, Research Institute of the McGill University Health Centre, Montréal General Hospital, Montréal, QC H3G 1A4, Canada
[6]Cancer Biology and Genetics, Memorial Sloan Kettering Cancer Center, New York, NY 10065, USA
[7]Department of Human Genetics, McGill University, Montréal, QC H3A 1A3, Canada
[8]Children's Hospital of Eastern Ontario Research Institute and Department of Biochemistry, Microbiology, and Immunology, University of Ottawa, Ottawa, ON K1H 8L1, Canada
[9]Patrick Wild Centre, Centre for Integrative Physiology, University of Edinburgh, Edinburgh EH8 9XD, UK
*Correspondence: xiang-jiao.yang@mcgill.ca (X.-J.Y.), nahum.sonenberg@mcgill.ca (N.S.)
http://dx.doi.org/10.1016/j.stem.2014.02.005

SUMMARY

Translational control plays a pivotal role in the regulation of the pluripotency network in embryonic stem cells, but its effect on reprogramming somatic cells to pluripotency has not been explored. Here, we show that eukaryotic translation initiation factor 4E (eIF4E) binding proteins (4E-BPs), which are translational repressors, have a multifaceted effect on the reprogramming of mouse embryonic fibroblasts (MEFs) into induced pluripotent stem cells (iPSCs). Loss of 4E-BP expression attenuates the induction of iPSCs at least in part through increased translation of *p21*, a known inhibitor of somatic cell reprogramming. However, MEFs lacking both p53 and 4E-BPs show greatly enhanced reprogramming resulting from a combination of reduced *p21* transcription and enhanced translation of endogenous mRNAs such as *Sox2* and *Myc* and can be reprogrammed through the expression of only exogenous *Oct4*. Thus, 4E-BPs exert both positive and negative effects on reprogramming, highlighting the key role that translational control plays in regulating this process.

INTRODUCTION

Transcription is suppressed during oocyte maturation and the initial divisions of the zygote, when the egg and sperm genomes undergo reprogramming (de Vries et al., 2008). Within this window of time, gene expression is largely controlled at the level of mRNA translation (Latham et al., 1991). Factor-induced reprogramming has primarily been linked to transcriptional and epigenetic events (Buganim et al., 2012; Gifford and Meissner, 2012). However, genome-wide analyses have indicated that the cellular proteome is mainly controlled at the translation level, and there is a limited correlation between mRNA and protein levels (Courtes et al., 2013; Lu et al., 2009; Schwanhäusser et al., 2011). The role of translational control in the reprogramming of somatic cells into induced pluripotent stem cells (iPSCs) has not been investigated.

Initiation is the rate-limiting step of translation and is subject to extensive control (Sonenberg and Hinnebusch, 2009). At this step, mRNA is recruited to the ribosome by the eukaryotic translation initiation factor 4F (eIF4F) complex, which consists of the cap binding protein eIF4E, the scaffolding protein eIF4G, and the RNA helicase eIF4A (Jackson et al., 2010). Although eIF4E is required for cap-dependent translation of all nuclear transcribed cellular mRNAs, it preferentially stimulates the translation of a subset of "eIF4E-sensitive" mRNAs, which includes mRNAs encoding proliferation- and survival-promoting proteins (Graff et al., 2008). The sensitivity of mRNA to eIF4E can be dictated by the structure and sequence of its 5′ untranslated region (5′ UTR) (Hsieh et al., 2012; Koromilas et al., 1992; Thoreen et al., 2012). The translation of mRNAs with long and structured 5′ UTRs is more dependent on eIF4E activity, and this can be explained by the stimulation of the eIF4A helicase activity by eIF4E (Feoktistova et al., 2013). The eIF4E binding proteins (4E-BP1, 4E-BP2, and 4E-BP3 in mammals) are translational inhibitors that, when dephosphorylated (activated), avidly bind eIF4E. The interactions of 4E-BPs with eIF4E prevent the association of eIF4E with eIF4G, which impair the assembly of the eIF4F complex (Pause et al., 1994; Poulin et al., 1998). The mammalian target of rapamycin complex 1 (mTORC1) phosphorylates (inactivates) the 4E-BPs, leading to their dissociation from eIF4E (Gingras et al., 1999; Gingras et al., 1998).

Notably, mTORC1-dependent phosphorylation of 4E-BPs is increased during embryonic stem cell (ESC) differentiation (Sampath et al., 2008), suggesting that 4E-BPs may also affect
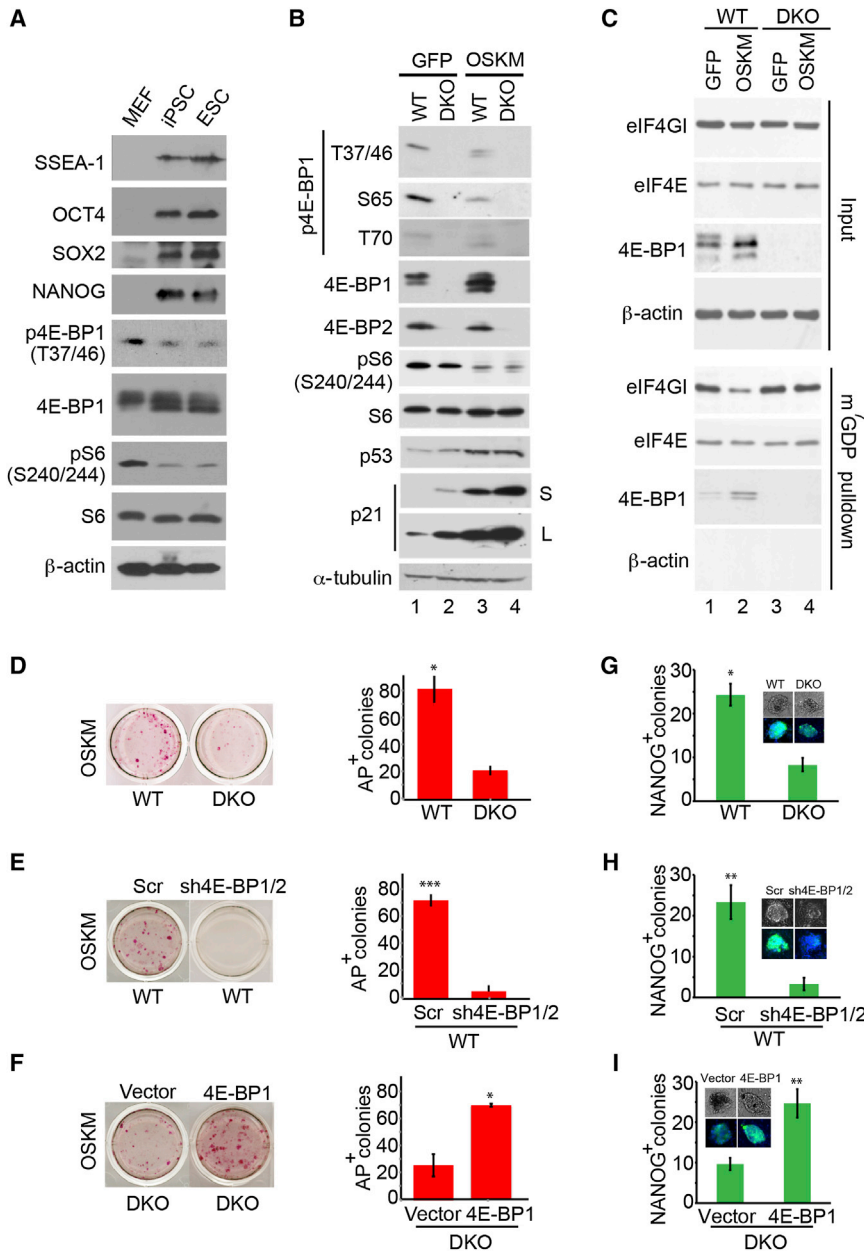
CrossMark

Figure 1. 4E-BPs Are Required for Somatic Cell Reprogramming

(A and B) Levels and phosphorylation status of the indicated proteins in ESCs (R1 clone), iPSCs (clone 9), and MEFs (A) or in WT and DKO MEFs infected with GFP or *Oct4*, *Sox2*, *Klf4*, and *Myc* (OSKM)-expressing lentiviral vectors and analyzed 7 days after the above transduction (B) were monitored by western blot. S, short exposure; L, long exposure.

(C) WT and DKO MEFs were infected with GFP- or OSKM-expressing viral vectors, and, on day 7 after infection, the cell extracts were subjected to m7GDP pull-down. Levels of the indicated proteins in the input (10%) or pull-down (25%) were determined by western blotting. β-actin served as a loading control (input) and to exclude nonspecific retention (m7GDP pull-down).

(D–F) WT and DKO MEFs (D), WT MEFs infected with scrambled shRNA (Scr) or shRNAs against 4E-BP1/4E-BP2 (sh4E-BP1/2; E), or DKO MEFs infected with a vector (control) or 4E-BP1 (F) were coinfected with OSKM. Reprogramming was monitored by AP staining on day 7 after OSKM infection. Data are presented as mean numbers of AP positive (AP[+]) colonies in bar charts SD (n = 3). *p < 0.05, ***p < 0.001; paired Student's t test.

(G–I) Reprogramming of MEFs described in (D–F) was monitored by NANOG immunofluorescence staining on day 14 after transduction. The NANOG immunofluorescence staining of a colony for each experimental condition are presented in the insets ± SD (n = 3). *p < 0.05, **p < 0.01; paired Student's t test.

See also Figure S1.

(OSKM) (Takahashi and Yamanaka, 2006). As expected, the phosphorylation of 4E-BP1 was markedly lower in iPSCs and ESCs in comparison to MEFs (He et al., 2012; Sampath et al., 2008) (Figure 1A). To ensure that the observed decrease in 4E-BP1 phosphorylation was not restricted to a subset of pluripotent cell lines, we monitored the phosphorylation levels of 4E-BP1 in various pluripotent cells whose pluripotency had been previously verified by chimeric contribution (Figure S1A available online). The cell lines include one ESC clone from B6CBAF1 mice (f-ESC), two ESC clones generated via somatic cell nuclear transfer (FNTESC and F-NtESC from B6;CBA and B6;129 genetic backgrounds, respectively), one ESC clone generated by parthenogenesis ([MII] ESC), and three iPSC clones derived from neural progenitor cells (NP-iPSCs), early hematopoietic progenitor cells (B-iPSC), and B-lymphocytes (BL-iPSC) (Hanna et al., 2008; Kim et al., 2011; Kim et al., 2010; Kim et al., 2007a; Kim et al., 2007b). 4E-BP1 phosphorylation was dramatically lower in all pluripotent cell lines in comparison to the MEFs (Figure S1A). Thus, low 4E-BP1 phosphorylation (high activity) is a salient feature of pluripotent cells, irrespective of their origin.

somatic cell reprogramming. Here, we demonstrate that eIF4E-dependent translational control via 4E-BPs plays an important role in regulating the factor-induced reprogramming. We also describe a crosstalk between the activity of 4E-BPs and the p53-p21 pathway in this process.
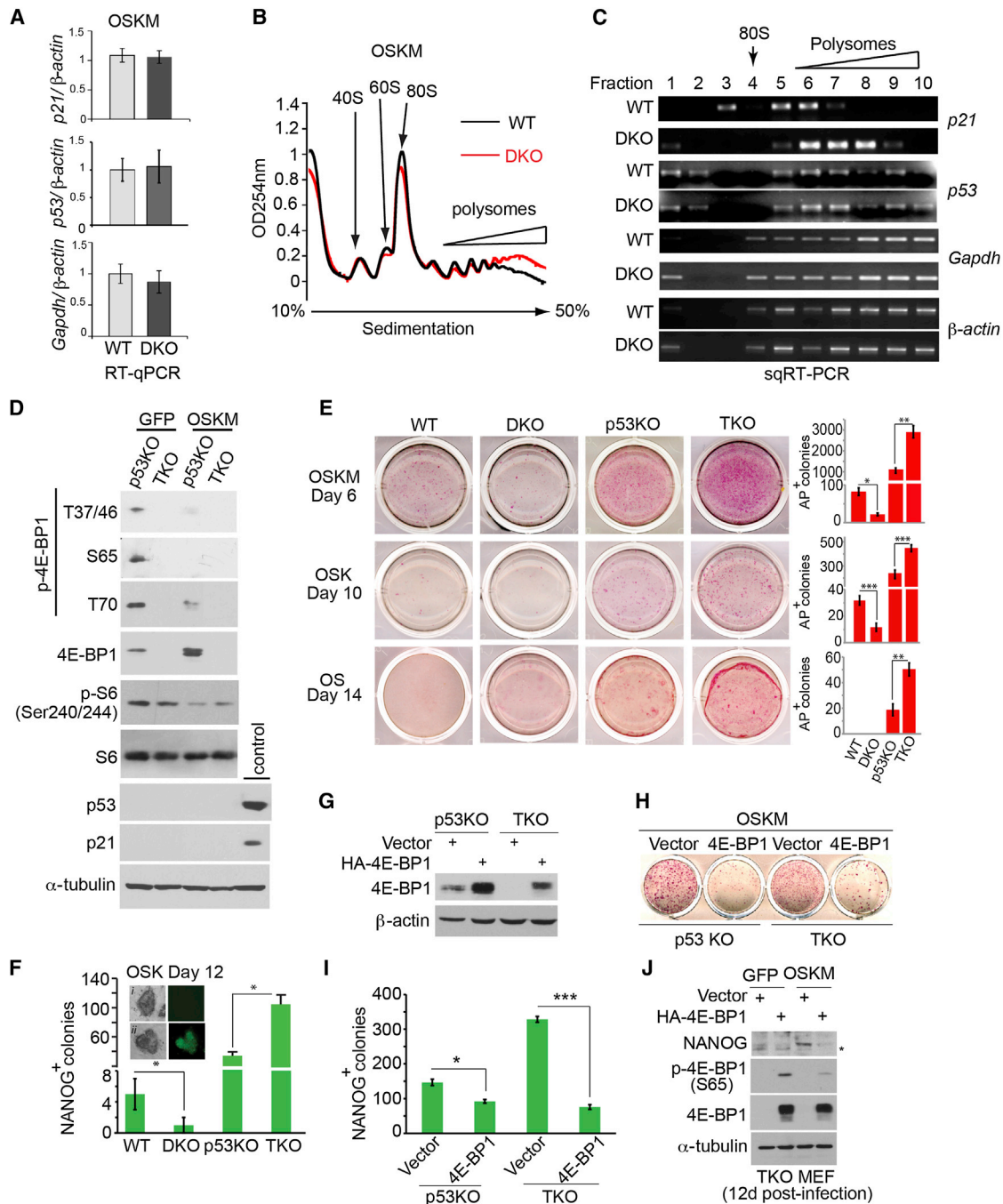
RESULTS

Activation of 4E-BP1 in Induced Pluripotent Stem Cells

To study the role of 4E-BPs in reprogramming, we first examined the phosphorylation status of 4E-BP1 in mouse embryonic fibroblasts (MEFs), mouse ESCs, and mouse iPSCs. iPSCs were generated by infecting wild-type (WT) MEFs with lentiviruses expressing the reprogramming factors *Oct4*, *Sox2*, *Klf4*, and *Myc*

Figure 2. Combined Loss of 4E-BPs and p53 Enhances Efficiency of Somatic Cell Reprogramming

(A) WT and DKO MEFs were infected with OSKM. At day 12 after infection, levels of the indicated mRNAs were determined by qRT-PCR. Data were normalized to β-actin mRNA, and the values for WT MEFs were set to 1. Results are presented as a mean ± SD (n = 3).

(B) Absorption profiles of ribosomes from cells described in (A). 40S and 60S denote the corresponding ribosomal subunits. 80S, monosome.

(C) Polysomal distribution of the indicated mRNAs in cells described in (A) were determined by semiquantitative RT-PCR (sqRT-PCR).

(D) Expression of the indicated proteins in GFP- or OSKM-infected p53KO and TKO MEFs was monitored by western blotting 7 days after infection. WT MEF lysates (control) served as a positive control for antibody specificity and α-tubulin as loading control.

(E) MEFs were infected with OSKM, OSK, or OS and reprogramming was monitored by AP staining at the indicated days after infection. Results are presented as a mean number of AP[+] colonies ± SD (n = 3). *p < 0.05, **p < 0.01, ***p < 0.001; paired Student's t test.

(F) MEFs were infected with OSK. At day 12 after infection immunofluorescence staining was used to detect NANOG[+] colonies. Results are presented as the mean number of NANOG[+] colonies in bar charts ± SD (n = 3). *p < 0.05; paired Student's t test. Representative micrographs of Nanog-negative (i) and -positive (ii) colonies are presented in the inset.

In addition to 4E-BPs, ribosomal protein S6 kinase 1 (S6K1) and S6K2 are major downstream targets of mTORC1 (Zoncu et al., 2011). Phosphorylation of ribosomal protein S6 (S6), which is a substrate of S6K1 and S6K2, was decreased in the pluripotent cells relative to MEFs, demonstrating that the activity of mTORC1 was lower in the pluripotent cells in comparison to MEFs (Figures 1A and S1A).

Essential Requirement of 4E-BPs in the Reprogramming of MEFs

Next, we focused on the role of 4E-BPs in the induction of pluripotency. First, we examined the phosphorylation of 4E-BP1 in MEFs transduced with OSKM. Phosphorylation of 4E-BP1 and S6 was markedly reduced early in reprogramming (Figure S1B). This result is consistent with a previous report that showed that intermediate stage reprogramming cells had lower mTORC1 activity than nonreprogramming cells (He et al., 2012). We also examined the role of 4E-BPs in reprogramming by expressing OSKM in WT and *4E-BP1/2*$^{-/-}$ (double knockout [DKO]) MEFs. The DKO MEFs are devoid of all 4E-BPs, given that 4E-BP3 is not expressed in MEFs (Dowling et al., 2010). Phosphorylation of S6 was not significantly different between the GFP-expressing WT and DKO MEFs (Figure 1B, lanes 1 and 2). Despite similar inhibition of mTORC1 signaling in the OSKM-expressing WT and DKO MEFs, as measured by the decrease in S6 phosphorylation (Figure 1B, lanes 3 and 4), the DKO MEFs formed significantly fewer primary iPSC colonies than the WT MEFs, as monitored by alkaline phosphatase (AP) and NANOG immunofluorescence staining (Figures 1D and 1G). Importantly, lentivirus infection efficiency and translation of *AP* and *Nanog* mRNAs were not affected by the 4E-BP status (Figures S1C–S1E and S2D). Although the DKO MEFs displayed a prolonged doubling time at later passages (passage ≥ 6), the defects in reprogramming cannot be explained by changes in the proliferation capacity of the DKO MEFs, given that early-passage MEFs (passage ≤ 3) were used for reprogramming and that doubling time of the DKO MEFs at early passages is similar to that of the WT MEFs (Petroulakis et al., 2009). To exclude the possibility that the attenuation of reprogramming in the DKO MEFs was caused by inadvertent changes that may have occurred during MEF isolation, we depleted 4E-BP1 and 4E-BP2 in WT MEFs (Figures 1E, 1H, and S1F) and re-expressed 4E-BP1 in the DKO MEFs (Figures 1F and 1I). Whereas depletion of the 4E-BPs attenuated reprogramming (Figures 1E and 1H), ectopic expression of 4E-BP1 rescued the reprogramming deficiency of the DKO MEFs, as determined by the increase in AP$^+$ and NANOG$^+$ colonies (Figures 1F and 1I). Notably, overexpression of WT 4E-BP1 in WT MEFs failed to promote reprogramming (Figures S1I–S1K). Altogether, these data demonstrate that 4E-BPs are necessary and required for the reprogramming of MEFs in a dose-dependent manner.

4E-BPs impede translation initiation by binding and sequestering eIF4E (Pause et al., 1994). To determine whether the binding of 4E-BPs to eIF4E is required for reprogramming, we expressed OSKM in DKO MEFs that harbor WT 4E-BP1 or a mutant lacking the eIF4E binding site (Δ4E-BS) (Rong et al., 2008). The number of AP$^+$ colonies formed by cells expressing the Δ4E-BS mutant was similar to that observed in control cells (DKO MEFs expressing vector) but was lower than that detected in cells expressing WT 4E-BP1 (Figure S1G). To investigate whether the ability of the 4E-BPs to inhibit eIF4F complex assembly correlates with the induction of reprogramming, we performed an m^{7}GDP-agarose pull-down assay (Figure 1C). Infection of WT MEFs with OSKM led to a reduction in eIF4F complex levels, as illustrated by the increase in the amount of 4E-BP1 and the decrease in the amount of eIF4GI pulled down by m^{7}GDP-agarose in comparison to GFP-infected cells 7 days after infection (Figure 1C, lanes 1 and 2). As expected, such a change did not occur in the OSKM-expressing DKO MEFs (Figure 1C, lanes 3 and 4). Collectively, these data identify an important function of 4E-BPs in promoting reprogramming by binding to eIF4E and disrupting eIF4F complex assembly on mRNAs encoding inhibitors of reprogramming.

Augmented Translation of *p21* mRNA in MEFs Lacking 4E-BP1 and 4E-BP2

In response to overexpression of reprogramming factors, cells activate the p53/p21 pathway to maintain genomic integrity during iPSC induction (Hong et al., 2009; Kawamura et al., 2009; Marión et al., 2009; Utikal et al., 2009). p21 acts as a major suppressor of somatic cell reprogramming (Hong et al., 2009), and cell types with higher reprogramming efficiency, such as keratinocytes, express relatively low levels of p21 protein (Kawamura et al., 2009). DKO MEFs express higher amounts of p21 protein in comparison to WT MEFs, and this disparity in p21 amounts was sustained 7 and 12 days after OSKM infection (Figures 1B and S2H). In contrast, no differences were found in *p21* mRNA levels between WT and DKO MEFs (Figure 2A). Similar to the DKO MEFs, downregulation of 4E-BP1 and 2 promotes the expression of p21 protein in MEFs (Figure S1H) (Kannan-Thulasiraman et al., 2008). Altogether, these findings indicate that 4E-BP-dependent regulation of *p21* mRNA translation plays an important role in reprogramming.

To further investigate the *p21* mRNA translation control, we performed a polysome profiling assay to directly examine whether the 4E-BPs suppress the translation initiation of *p21* mRNA during reprogramming (Figure 2B). Polysomes from OSKM-infected WT and DKO MEFs (12 days after infection) were fractionated with sucrose density gradients. In this assay, mRNAs whose translation initiation is efficient are associated with heavy polysomes, and they sediment faster than poorly

(G) Western blot analysis of 4E-BP1 in p53KO MEFs and TKO MEFs infected with HA-4E-BP1 or vector and treated with puromycin (5 μg/ml) for 7 days. β-actin served as the loading control.

(H and I) Cells described in (G) infected with OSKM and seeded on feeder layer. At day 12 after infection, reprogramming of MEFs was monitored by AP staining (H) or NANOG immunofluorescence staining (I). Results are presented as a mean number of NANOG$^+$ colonies ± SD (n = 3). *p < 0.05, ***p < 0.001; paired Student's t test.

(J) Western blot analysis of NANOG, 4E-BP1, and p-4E-BP1(S65) in TKO MEFs expressing vector or HA-4E-BP1 12 days after infection with GFP or OSKM. The asterisk represents nonspecific band.

See also Figure S2.

translated mRNAs, which are associated with light polysomes (Warner et al., 1963). The absorbance profiles of the gradient fractions indicated a modest increase in global translation in the OSKM-infected DKO MEFs relative to the WT MEFs, as judged by an increase in polysome content with a concomitant decrease in the 80S peak (Figure 2B). Significantly, *p21* mRNA was preferentially associated with heavier polysomes in the DKO MEFs (fractions 6–8) in comparison to the WT MEFs, in which *p21* mRNA was associated with lighter polysomes (fractions 5–6; Figure 2C; Figure S2A). In sharp contrast, the positions of the *p53*, *Gapdh*, *β-actin*, and *Nanog* mRNAs were not affected by the 4E-BP status (Figures 2C and S2B–S2D). Altogether, these results demonstrate that 4E-BPs selectively suppress the translation of *p21* mRNA and that the reduced reprogramming efficiency of the DKO MEFs stems from their inability to suppress *p21* mRNA translation. This conclusion is supported by the finding that p21 depletion partially alleviated the inhibition of reprogramming in DKO MEFs (Figures S2E–S2G). However, it is highly likely that other eIF4E-sensitive genes are also involved, given that the depletion of p21 could not fully rescue the reprogramming deficiency of the DKO MEFs.

p53 Loss Reverses the Effects of 4E-BPs on Somatic Cell Reprogramming

p53 inhibits reprogramming largely by activating *p21* transcription (Hong et al., 2009; Kawamura et al., 2009; Marión et al., 2009; Utikal et al., 2009). As expected, due to the loss of p53 expression, *p21* mRNA and protein were barely detectable in *p53$^{-/-}$* (p53KO) and *p53$^{-/-}$;4E-BP1/2$^{-/-}$* (TKO) MEFs (Figure 2D and S2H–S2J). Therefore, we reasoned that the loss of p53 expression should rescue the feeble reprogramming caused by the loss of 4E-BP expression. To investigate this hypothesis, we expressed reprogramming factors in the WT, DKO, p53KO, and TKO MEFs and monitored reprogramming efficiency. Consistent with previous reports (Hong et al., 2009; Kawamura et al., 2009; Marión et al., 2009; Utikal et al., 2009), reprogramming efficiency, as determined by the number of AP$^+$ and NANOG$^+$ colonies, was higher in the p53KO MEFs than it was in the WT MEFs (Figures 2E and 2F). Surprisingly, the number of iPSC colonies formed by the TKO MEFs was significantly higher than that formed by the p53KO MEFs (mean = 1,107 AP$^+$ colonies in the OSKM-expressing p53KO MEFs versus 2,915 AP$^+$ colonies in the OSKM-expressing TKO MEFs; p = 0.003) (Figures 2E and 2F). These effects were not a consequence of differences in the infection efficiency between the p53KO and TKO MEFs (Figures S2K and S2L). Importantly, these effects were p53 dependent, given that p53 re-expression in the TKO MEFs led to increased p21 protein amounts and suppressed reprogramming (Figures S2M and S2N). As expected, overexpression of 4E-BP1 in the p53KO and TKO MEFs inhibited reprogramming with a more significant effect on the TKO MEFs (Figures 2G–2J). An increase in the number of primary iPSC colonies in the TKO MEFs, relative to the p53KO MEFs, was also detected in cells infected with OSK or OS (Figures 2E and 2F). Remarkably, the expression of *Oct4* alone was sufficient to generate iPSCs from the TKO MEFs (Figures S3A and S3B), albeit at a very small number (two to ten expandable iPSC colonies per 40,000 *Oct4*-infected TKO MEFs in three experiments) but not from the p53KO MEFs. *Oct4*-induced TKO iPSCs

(Oct4-TKO-iPSCs) maintained the expression of ESC specific markers, such as *Nanog*, *Rex1*, and stage-specific embryonic antigen 1 (Figures 3A–3C and S3C), and differentiated into cells originating from all three germ layers, including functional neurons, blood vessels, muscle, bone, adipose, and gut-like tissues in teratoma and embryoid body formation assays (Figures 3D–3H and 4A–4C).

Next, we determined the ability of the Oct4-TKO-iPSCs to produce chimeric offspring. The loss of p53 leads to aneuploidy and therefore dramatically decreases the efficacy of chimera generation (Menendez et al., 2010). To circumvent this problem, we selected a clone of the Oct4-TKO-iPSCs that was devoid of alterations in chromosome number (Oct4-TKO-iPSC-11; Figure S4A) and expressed enhanced GFP (eGFP$^+$). This clone was injected into mouse blastocysts. Oct4-TKO-iPSC-11 contributed to the generation of chimeras, as evident in the prenatal embryos, live-born neonates, and young pups (Figures 4D and S4B–S4D and Table S1). Chimeras were scored with eGFP fluorescence at the whole-body surface level of the embryonic day 14.5 (E14.5) embryos (Figure 4Di), and the 24 hr old neonates (Figure 4Dii) or as the mosaic colored chimeras in young pups (Figure 4Diii). Chimera contribution was also quantified as eGFP fluorescence in the whole body of ten independent E14.5–E16.5 prenatal chimeric embryos (Figure S4B and Table S1) and organs such as heart, liver, and gonads (testis) of E16.5 chimeric embryos (Figure S4C). Germline competency was also confirmed by the presence of both eGFP$^+$ and THY-1$^+$ gonadal cells (Figure S4D) and the chimera-derived offspring. Collectively, these data demonstrate that Oct4-TKO-iPSCs are fully reprogrammed and pluripotent.

Translation of *Sox2* and *Myc* mRNAs Is Induced in the Oct4-Expressing TKO MEFs

At the molecular level, mTORC1 signaling was suppressed to a comparable extent in the OSKM-expressing p53KO and TKO MEFs, as illustrated by a comparable reduction in the phosphorylation of S6 (Figure 2D). Consistent with the findings observed in the WT and DKO MEFs (Figure 1C), eIF4F complex assembly was attenuated in the OSKM-infected p53KO MEFs but not in GFP-infected p53KO or TKO MEFs (Figure 5A). Also, global translation was modestly increased in Oct4-infected TKO MEFs in comparison to p53KO MEFs, as implied by the polysome profiling results (Figure 5B). These data indicate that the loss of 4E-BP expression in a p53-null background stimulates iPSC generation via a selective increase in the translation of mRNAs encoding factors that stimulate reprogramming. Indeed, *Myc* and *Sox2* mRNAs sedimented with heavy polysomes in the Oct4-infected TKO MEFs in comparison to the Oct4-infected p53KO MEFs, whereas there was no difference in the sedimentation of *Klf4*, *Gapdh*, and *β-actin* mRNAs (Figures 5C and S5A–S5D). These findings are consistent with previous reports demonstrating that the translation of *Myc* and *Sox2* mRNAs is eIF4E dependent (De Benedetti and Graff, 2004; Ge et al., 2010; Stoyanova et al., 2013). Accordingly, the levels of MYC and SOX2 proteins were upregulated in the Oct4-infected TKO MEFs and coincided with the induction of NANOG expression (Figure 5D). In stark contrast, NANOG was not expressed in Oct4-infected p53KO MEFs (Figure 5D). The absence of 4E-BP expression failed to cause a shift of *Nanog* mRNA to heavy
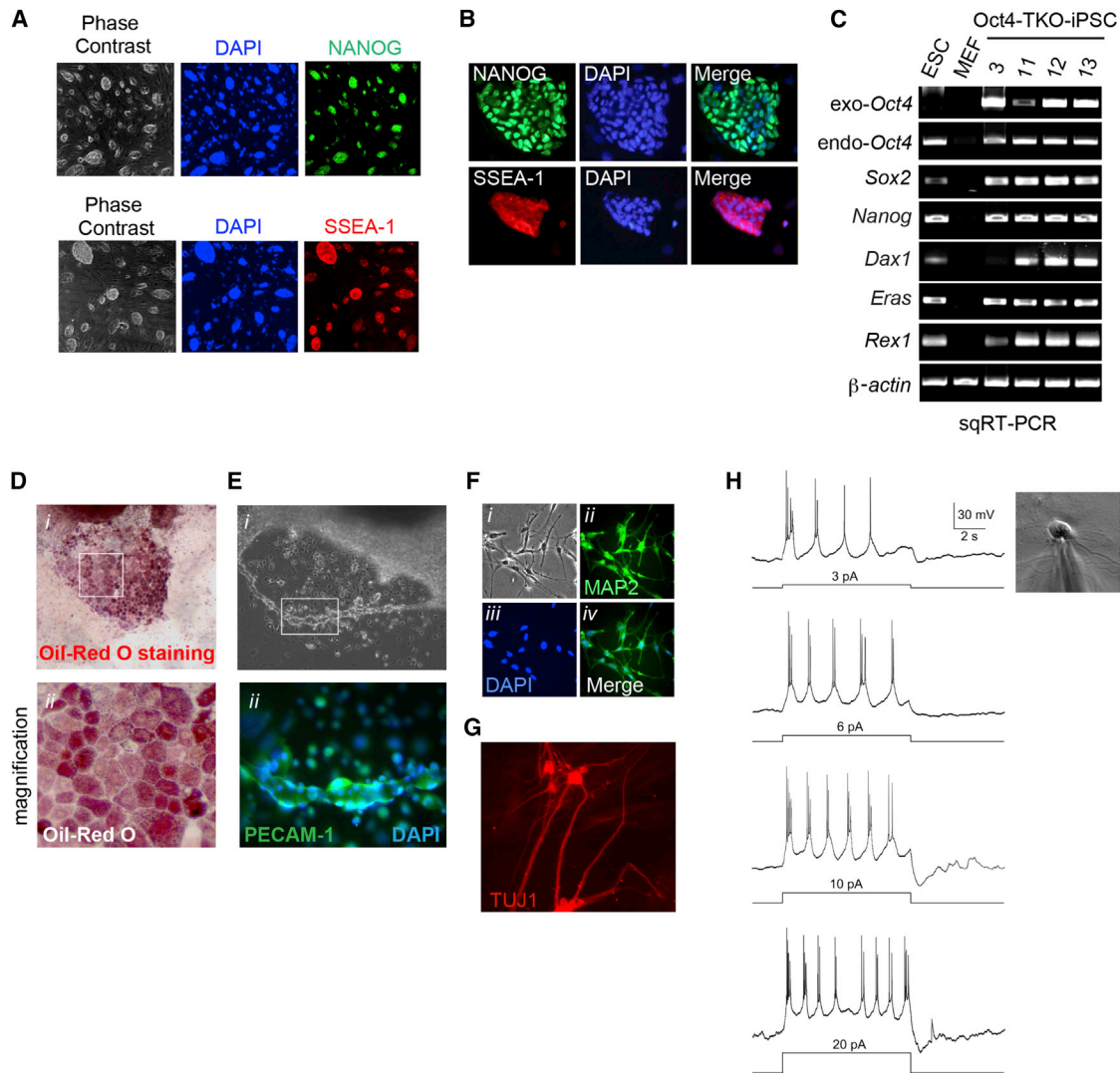
Figure 3. Characterization and Differentiation of Oct4-Induced TKO iPSCs

(A) Micrographs representing phase contrast, NANOG (green), and SSEA-1 (red) immunofluorescence staining images of Oct4-induced TKO iPSC clone 11 (Oct4-TKO-iPSC-11). Nuclei were counterstained with DAPI (blue).

(B) NANOG and SSEA-1 immunofluorescence staining of individual Oct4-induced TKO iPSC clone 1 (Oct4-TKO-iPSC-1). Nuclei were counterstained with DAPI (blue).

(C) Exogenous and endogenous levels of the indicated ESC marker mRNAs were monitored in four independent Oct4-TKO-iPSC clones by sqRT-PCR.

(D–H) Differentiation of Oct4-TKO-iPSC-1- and Oct4-TKO-iPSC-3-derived embryoid bodies into adipocytes (D), blood vessels (E), and functional neurons (F–H). Oil-Red O staining of adipocytes (D*i*). Phase-contrast image of blood vessels (E*i*). Regions marked with white squares in (D*i*) and (E*i*) are magnified 10× in (D*ii*) and (E*ii*). Immunofluorescence staining of platelet endothelial cell adhesion molecule (PECAM-1, green), and DAPI staining of nuclei (blue) of blood vessels (E*ii*).

(F) Micrographs represent phase-contrast image (*i*), microtubule-associated protein 2 (MAP2) immunofluorescence staining (green, *ii*), nuclear staining with DAPI (blue; *iii*), and overlay of MAP2 and DAPI staining *(iv)*.

(G) Neuron-specific class III β-tubulin immunofluorescence staining with anti-TUJ1.

(H) Whole-cell current clamp recordings from neurons derived from Oct4-TKO-iPSC-3. Traces show representative recordings from cells generating action potentials in response to step depolarization elicited by current injection (n = 10). Membrane potential was current clamped at around −65 mV. The scale bar applies to all traces. Phase contrast image of Oct4-TKO-iPSC-derived neurons with patch electrode is displayed on right top corner.

See also Figure S3.

polysomes (Figure S2D), thereby indicating that the observed increase in NANOG protein in Oct4-expressing TKO MEFs was mediated through the induction of *Nanog* transcription (Figure S5F) rather than by the stimulation of *Nanog* mRNA translation. Intriguingly, although forced expression of *Oct4* failed to stimulate the translation of *Klf4* mRNA in a 4E-BP-dependent manner (Figures 5C and S5B), it resulted in a strong induction of *Klf4* mRNA and protein expression in both the p53KO and TKO cells (Figures 5D and 5E). However, the upregulation of *Klf4* expression was not sufficient to reprogram Oct4-infected p53KO MEFs, indicating that increased translation of *Sox2* and *Myc* mRNAs plays a crucial role in the induction of pluripotency
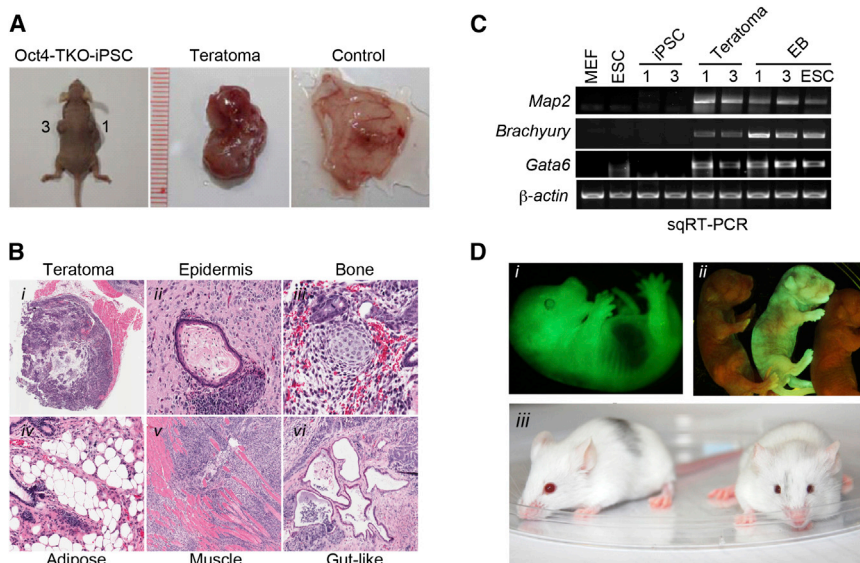
Figure 4. Oct4-Induced TKO iPSC Clones Are Pluripotent and Contribute to Chimeric Mouse Offspring

(A) Teratoma formation assay with two independent Oct4-induced TKO-iPSC clones (Oct4-TKO-iPSC clones 1 and 3). TKO MEFs were used as negative control in the teratoma formation assay.

(B) Hematoxylin and eosin staining of a teratoma (*i*) derived from Oct4-TKO-iPSC-1. Sections from a Oct4-TKO-iPSC-1-derived teratoma represent all three embryonic germ-layer tissues namely ectoderm (epidermis, *ii*), mesoderm (bone, *iii*; adipose tissue, *iv*; and muscle, *v*), and endoderm (gut-like tissue, *vi*).

(C) sqRT-PCR analysis of *Map2* (neuroectodermal lineage marker), *Brachyury* (mesodermal lineage marker), or *Gata6* (endodermal lineage marker) mRNA levels in MEFs, ESCs, Oct4-TKO-iPSC clones 1 and 3, and teratomas and EBs derived from Oct4-TKO-iPSC clones 1 and 3 or ESCs. *β-actin* mRNA served as a loading control.

(D) Fluorescence imaging of eGFP in chimeras of prenatal embryos (E14.5, *i*) and neonates (24 hr old, *ii*) and the bright-field images of coat color appearance (*iii*) in the adult chimeras, where all were generated by injection of Oct4-TKO-iPSC-11 into mouse blastocysts. The level of chimeric contribution in (*ii*, from left to right) ranges from a sparsely mosaic chimera to an extensively mosaic chimera and a nonchimeric control.

See also Figure S4 and Table S1.

in the TKO MEFs. Notably, similar to the TKO MEFs, overexpression of *Oct4* alone is sufficient to reprogram neural stem cells, which exhibit high endogenous expression of SOX2 and MYC proteins (Kim et al., 2009b, 2009c). Altogether, these results support a model whereby Oct4-induced reprogramming of TKO MEFs requires optimal orchestration of reprogramming factor expression via 4E-BP-dependent (*Myc* and *Sox2*) and independent (*Klf4*) mechanisms to engender a favorable stoichiometry of the reprogramming factors (Carey et al., 2011).

DISCUSSION

A large body of evidence shows that transcriptional and epigenetic mechanisms govern the generation of iPSCs (Gifford and Meissner, 2012; Jaenisch and Young, 2008). The incorporation of a 5′ guanine cap analog (an antireverse diguanosine cap analog) and a strong translational initiation signal into synthetic mRNAs encoding reprogramming factors significantly enhanced mRNA stability and translation efficiency (Warren et al., 2010). Repeated transfection of the modified mRNAs dramatically increased iPSC generation, suggesting that translational control plays an important role in somatic cell reprogramming (Warren et al., 2010). In addition, several studies demonstrated that the administration of ESC-specific microRNAs could substitute for some of the reprogramming factors and enhance iPSC generation (Judson et al., 2009; Subramanyam et al., 2011). microRNAs are small noncoding RNAs that posttranscriptionally repress their target genes through mRNA degradation or translational repression (Fabian et al., 2010). These studies suggest that the balance between the translation of the reprogramming-stimulatory and -inhibitory factors plays an important role in effecting the outcome of reprogramming.

Herein, we documented a layer of regulation via 4E-BP-mediated translational control of the mRNAs encoding p21, SOX2, and MYC. We have not examined the contribution of other translational control mechanisms, such as S6Ks or eIF2α, in the regulation of somatic cell reprogramming. Our data demonstrate that forced expression of reprogramming factors represses eIF4E-dependent translation through the dephosphorylation of 4E-BPs. Consistent with this finding, a previous study showed that 4E-BP1 acts as a molecular switch during ESC differentiation (Sampath et al., 2008). Whereas undifferentiated ESCs maintain 4E-BP1 in a hypophosphorylated and active state, differentiation induces 4E-BP1 phosphorylation and promotes the translation of differentiation-inducing mRNAs. This finding is reminiscent of a transcriptionally poised state of the developmental genes in ESCs, which repress the transcription of differentiation-inducing genes (Bernstein et al., 2006). The genome-wide cross-talk between transcription and translation during reprogramming and differentiation remains to be examined (Lu et al., 2009).

Our results also reveal a functional interplay between 4E-BPs and the p53-p21 pathway, which affects the synchronization of the transcriptional and translational programs and is essential for reprogramming (Figure 5F). Accordingly, cells divide more rapidly at a smaller size than that of fibroblasts during early stages of reprogramming (Smith et al., 2010). This apparent loss of the cell-size checkpoint control in reprogramming cells parallels the ability of the TKO MEFs to attain constant proliferation rates independent of their size (Dowling et al., 2010). It is noteworthy that the better reprogramming of the TKO MEFs is not due to higher proliferation rates, given that p53KO MEFs proliferate at the same rate as the TKO MEFs (Dowling et al., 2010). These findings demonstrate that a combined loss of 4E-BPs and p53 expression may alleviate the restraining effects of cell-sizing mechanisms during reprogramming.

4E-BPs play a bimodal role during reprogramming. In WT MEFs, forced expression of reprogramming factors overcomes the inhibitory effect of 4E-BPs on *Sox2* and *Myc* mRNA
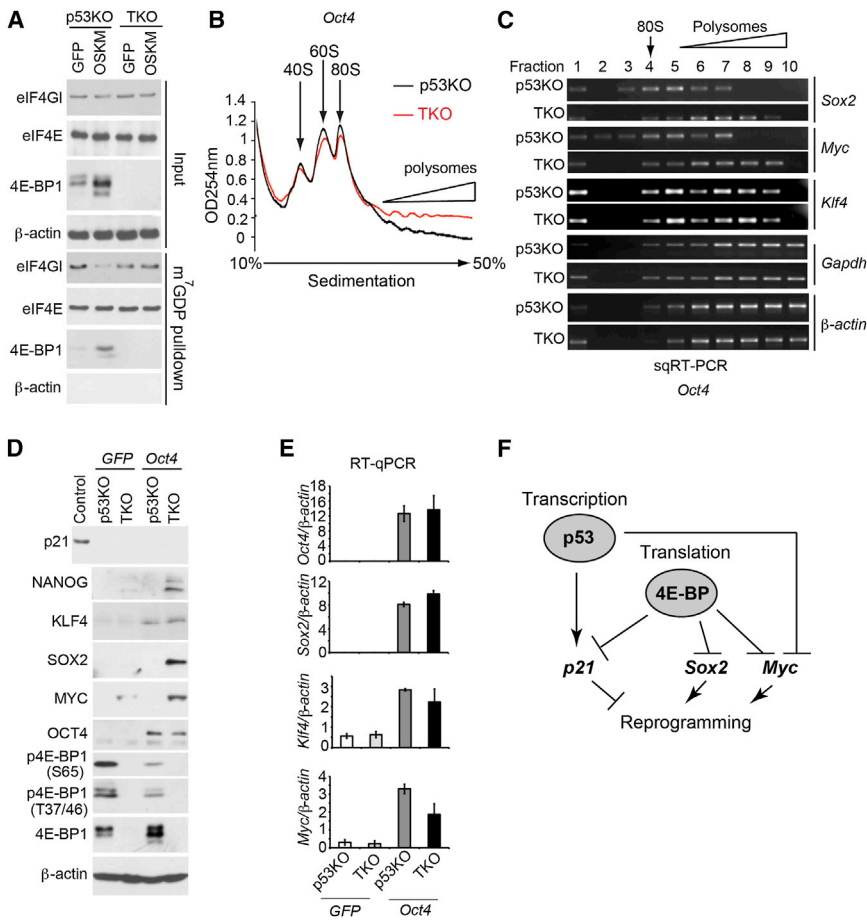
Figure 5. Increased Translation of *Sox2* and *Myc* mRNAs and Downregulated p21 Expression Correlate with High Reprogrammability of TKO MEFs

(A) p53KO and TKO MEFs were infected with GFP or OSKM expression lentivectors. At day 7 after infection, cell extracts were subjected to m⁷GDP pull-down. Levels of the indicated proteins in the input (10%) or pull-down (25%) samples were determined by western blotting. β-actin served as a loading control (input) and to exclude nonspecific binding (m⁷GDP pull-down).

(B) Absorption profiles of ribosomes from p53KO and TKO MEFs 12 days after infection with *Oct4* expressing lentivector. 40S and 60S denote the corresponding ribosomal subunits. 80S, monosome.

(C) Polysomal distributions of *Sox2*, *Myc*, *Klf4*, *Gapdh*, and *β-actin* mRNAs in cells described in (B) were determined by sqRT-PCR.

(D) Expression of the indicated proteins in cells described in (B) was monitored by western blotting. WT MEF lysates (control) and β-actin served as a positive and loading control, respectively.

(E) Levels of the indicated mRNAs from cells described in (B) were monitored by qRT-PCR. Values were normalized to *β-actin* mRNA and presented in arbitrary units. Results are presented as mean ± SD (n = 3).

(F) Model showing the link between p53/p21 pathway and 4E-BP-dependent translational control in factor-induced reprogramming.

See also Figure S5.

translation, whereas endogenous *p21* mRNA translation is suppressed. The 4E-BP DKO cells, in which the translation of *p21* mRNA is not repressed, are resistant to reprogramming. In TKO MEFs, a combination of downregulated *p21* mRNA expression and increased translation of the *Sox2* and *Myc* mRNAs caused by the loss of p53 and 4E-BPs, respectively, results in increased reprogramming efficiency. In this regard, overexpression of *Cyclin D1*, a well-established target of eIF4E (Rosenwald et al., 1993), enhances somatic cell reprogramming (Tanabe et al., 2013). Interestingly, *Cyclin D1* overexpression synergizes with p53 suppression to promote human iPSC generation (Edel et al., 2010; Tanabe et al., 2013). This finding suggests that, in addition to *Myc* and *Sox2*, other eIF4E-sensitive mRNAs contribute to the enhanced reprogramming efficiency of TKO MEFs. Genome-wide translatome analysis is required to identify these additional targets.

The current methods for iPSC generation are based on the forced expression of exogenous reprogramming factors via various methods, including viral infection, plasmid transfection, transposition systems, and the delivery of mRNAs, recombinant proteins, or small molecules (Anokye-Danso et al., 2011; Han et al., 2012; Hou et al., 2013; Kim et al., 2009a; Okita et al., 2008; Stadtfeld et al., 2008; Warren et al., 2010; Zhou et al., 2009). Our findings raise the possibility that targeted manipulation of translation of mRNAs encoding factors that govern pluripotency could be considered in devising more efficient protocols

for the production of iPSCs. Follow-up studies are required in order to examine the effects of eIF4E-dependent translation on human somatic cell reprogramming and develop clinically compatible iPSCs for prospective therapeutic applications.

EXPERIMENTAL PROCEDURES

The Animal Ethics Committee of the McGill University approved all the animal procedures.

Polysome Fractionation Analysis, RNA Isolation, and RT-PCR

For polysome analysis, MEFs were infected with lentiviruses expressing OSKM (only *Oct4* in Figures 5B and 5C) or GFP and cultured in two 15 cm dishes for 12 days. Then, 100 μg/ml cycloheximide was added to the media, and MEFs were washed twice with ice-cold PBS containing 100 μg/ml cycloheximide, collected by scrapping, and lysed in a hypotonic lysis buffer (5 mM Tris-HCl [pH 7.5], 2.5 mM MgCl₂, 1.5 mM KCl, 100 μg/ml cycloheximide, 2 mM dithiothreitol [DTT], 0.5% Triton X-100, and 0.5% sodium deoxycholate). Lysates were loaded onto buffered 10%–50% sucrose density gradients (20 mM HEPES-KOH [pH 7.6], 100 mM KCl, and 5 mM MgCl₂) and centrifuged at 36,000 rpm for 2 hr at 4°C in an SW41 rotor (Beckman Coulter). Gradients were fractionated, and optical density at 254 nm was continuously recorded with a FOXO JR Fractionator (Teledyne Isco). RNA from each fraction was isolated with Trizol reagent (Invitrogen) according to the manufacturer's instructions. RT-PCR reactions were carried out with Expand Reverse Transcriptase (Roche) for complementary DNA synthesis and Taq DNA Polymerase (Fermentas) according to the manufacturer's instructions. The primers used for each transcript are listed in the Supplemental Experimental Procedures. To ensure that the reactions were in the linear (quantifiable) range, RT-PCR assays were

performed under the same conditions with a serial dilution of RNA isolated from WT MEFs (Figure S5E). Quantitative RT-PCR was performed with 2× SYBR Green Master Mix (Applied Biosystems) and PCR Mastercycler (Eppendorf).

Cap Pull-Down Assay

MEFs were seeded in two 10 cm plates and infected with OSKM or GFP. Cells were washed with ice-cold PBS, collected by scrapping, and lysed in buffer A (50 mM MOPS/KOH [pH 7.4], 100 mM NaCl, 50 mM NaF, 1 mM Na_3VO_4, 2 mM EDTA, 2 mM EGTA, 1% NP40, 1% Na-deoxycholate, 7 mM β-mercaptoethanol, and EDTA-free protease inhibitor cocktail from Roche) 7 days postinfection. Lysates were precleared by centrifugation (12,000 × g for 10 min), diluted to 0.5 mg/ml with buffer B (50 mM MOPS/KOH [pH 7.4], 100 mM NaCl, 50 mM NaF, 1 mM Na_3VO_4, 0.5 mM EDTA, 0.5 mM EGTA, 7 mM β-mercaptoethanol, 0.1 mM GDP, and EDTA-free protease inhibitor cocktail from Roche) and incubated with m^7GDP-agarose beads (homemade) for 20 min at 4°C. After incubation, beads were washed three times with buffer B, eluted with 0.2 mM m^7GDP, resuspended in SDS-PAGE loading buffer, and analyzed by western blotting.

Virus Generation and Infections

Lentiviruses expressing reprogramming factors were produced in human embryonic kidney (HEK) 293FT cells by cotransfection of the helper constructs (psPAX2 and pMD2.G) with pLOVE-Klf4, pLOVE-N-myc, pSin-EF2-Sox2-Pur, or pSin-EF2-Oct4-Pur (Blelloch et al., 2007; Yu et al., 2007). pLOVE-GFP was used as a control (plasmid 15949, Addgene). Retroviral infections with pBABE-HA-(WT) 4E-BP1 or Δ4E-BP mutant were carried out as described previously (Rong et al., 2008). pLKO-4E-BP1 and 4E-BP2 small hairpin RNAs (shRNAs) were purchased from Sigma-Aldrich (TRCN0000075612 [shBP1] and TRCN0000075614 [shBP2]). Lentivirus generation and infection were carried out as described previously (Dowling et al., 2010). The generation of adenoviruses expressing GFP and p53 and infection conditions has been described previously (Petroulakis et al., 2009). Addgene plasmid 24129 (pUltra) was used for eGFP labeling of Oct4-TKO-iPSCs. The lentiviral supernatant was prepared by cotransfection of pUltra, pCMV-d8.91, and pMD2.G into HEK293T cells (Dogan et al., 2010) and transduced into the Oct4-TKO-iPSCs (passage 3).

MEF-to-iPSC Reprogramming

Mouse iPSCs were generated as described previously (Blelloch et al., 2007). MEFs were seeded into 12-well tissue culture dishes at 4×10^4 cells per well and incubated with a virus mixture in presence of 8 μg/ml of polybrene for 48 hr. Mouse ESC medium (Dulbecco's modified Eagle's medium [Invitrogen], 1% nonessential amino acids [Invitrogen, 100× stock], 1% GlutaMAX-1 [Invitrogen, 100× stock], 1% sodium pyruvate [100× stock from Invitrogen], 0.1 mM β-mercaptoethanol, 15% fetal bovine serum, 1,000 U mouse LIF/ml [ESGRO, Millipore], penicillin [50 μg/ml], and streptomycin [50 μg/ml]) was used to maintain the cells after infection. Medium was changed every second day. For alkaline phosphatase staining, an alkaline phosphatase detection kit (Millipore) was used according to the manufacturer's instruction. Data are presented as mean ± SD. Paired Student's t tests were performed to calculate p value.

Electrophysiology Studies

iPSC-derived neurons were flooded with HEPES-buffered saline containing 140 mM NaCl, 3 mM KCl, 1 mM MgCl2, 10 mM HEPES, 1 mM CaCl2, and 10 mM glucose. Neurons were patch clamped with glass pipettes (1.2 mM outer diameter glass, A-M Systems) containing a solution comprising 120 mM K-gluconate, 10 mM HEPES, 1 mM MgCl2, 4 mM Na-ATP, and 10 mM EGTA (pH 7.1) adjusted with KOH. Whole-cell recordings were performed with an Axopatch-1D Patch Clamp Amplifier (Molecular Devices) and digitized (10 kHz) via a Digidata 1200B interface coupled to a computer running Clampex 8 (Molecular Devices). Membrane potentials were kept around −60 to −70 mV, and step currents were injected to elicit action potential.

SUPPLEMENTAL INFORMATION

Supplemental Information contains Supplemental Experimental Procedures, five figures, and one table and can be found with this article online at http://dx.doi.org/10.1016/j.stem.2014.02.005.

REFERENCES

Anokye-Danso, F., Trivedi, C.M., Juhr, D., Gupta, M., Cui, Z., Tian, Y., Zhang, Y., Yang, W., Gruber, P.J., Epstein, J.A., and Morrisey, E.E. (2011). Highly efficient miRNA-mediated reprogramming of mouse and human somatic cells to pluripotency. Cell Stem Cell 8, 376–388.

Bernstein, B.E., Mikkelsen, T.S., Xie, X., Kamal, M., Huebert, D.J., Cuff, J., Fry, B., Meissner, A., Wernig, M., Plath, K., et al. (2006). A bivalent chromatin structure marks key developmental genes in embryonic stem cells. Cell 125, 315–326.

Blelloch, R., Venere, M., Yen, J., and Ramalho-Santos, M. (2007). Generation of induced pluripotent stem cells in the absence of drug selection. Cell Stem Cell 1, 245–247.

Buganim, Y., Faddah, D.A., Cheng, A.W., Itskovich, E., Markoulaki, S., Ganz, K., Klemm, S.L., van Oudenaarden, A., and Jaenisch, R. (2012). Single-cell expression analyses during cellular reprogramming reveal an early stochastic and a late hierarchic phase. Cell 150, 1209–1222.

Carey, B.W., Markoulaki, S., Hanna, J.H., Faddah, D.A., Buganim, Y., Kim, J., Ganz, K., Steine, E.J., Cassady, J.P., Creyghton, M.P., et al. (2011). Reprogramming factor stoichiometry influences the epigenetic state and biological properties of induced pluripotent stem cells. Cell Stem Cell 9, 588–598.

Courtes, F.C., Lin, J., Lim, H.L., Ng, S.W., Wong, N.S., Koh, G., Vardy, L., Yap, M.G., Loo, B., and Lee, D.Y. (2013). Translatome analysis of CHO cells to identify key growth genes. J. Biotechnol. 167, 215–224.

De Benedetti, A., and Graff, J.R. (2004). eIF-4E expression and its role in malignancies and metastases. Oncogene 23, 3189–3199.

de Vries, W.N., Evsikov, A.V., Brogan, L.J., Anderson, C.P., Graber, J.H., Knowles, B.B., and Solter, D. (2008). Reprogramming and differentiation in mammals: motifs and mechanisms. Cold Spring Harb. Symp. Quant. Biol. 73, 33–38.

Dogan, Y., Ganser, A., Scherr, M., and Eder, M. (2010). Quantification of transforming capacity and cooperation of defined genetic alterations in myeloid malignancies. Exp. Hematol. 38, 11–19.

Dowling, R.J., Topisirovic, I., Alain, T., Bidinosti, M., Fonseca, B.D., Petroulakis, E., Wang, X., Larsson, O., Selvaraj, A., Liu, Y., et al. (2010). mTORC1-mediated

cell proliferation, but not cell growth, controlled by the 4E-BPs. Science *328*, 1172–1176.

Edel, M.J., Menchon, C., Menendez, S., Consiglio, A., Raya, A., and Izpisua Belmonte, J.C. (2010). Rem2 GTPase maintains survival of human embryonic stem cells as well as enhancing reprogramming by regulating p53 and cyclin D1. Genes Dev. *24*, 561–573.

Fabian, M.R., Sonenberg, N., and Filipowicz, W. (2010). Regulation of mRNA translation and stability by microRNAs. Annu. Rev. Biochem. *79*, 351–379.

Feoktistova, K., Tuvshintogs, E., Do, A., and Fraser, C.S. (2013). Human eIF4E promotes mRNA restructuring by stimulating eIF4A helicase activity. Proc. Natl. Acad. Sci. USA *110*, 13339–13344.

Ge, Y., Zhou, F., Chen, H., Cui, C., Liu, D., Li, Q., Yang, Z., Wu, G., Sun, S., Gu, J., et al. (2010). Sox2 is translationally activated by eukaryotic initiation factor 4E in human glioma-initiating cells. Biochem. Biophys. Res. Commun. *397*, 711–717.

Gifford, C.A., and Meissner, A. (2012). Epigenetic obstacles encountered by transcription factors: reprogramming against all odds. Curr. Opin. Genet. Dev. *22*, 409–415.

Gingras, A.C., Kennedy, S.G., O'Leary, M.A., Sonenberg, N., and Hay, N. (1998). 4E-BP1, a repressor of mRNA translation, is phosphorylated and inactivated by the Akt(PKB) signaling pathway. Genes Dev. *12*, 502–513.

Gingras, A.C., Gygi, S.P., Raught, B., Polakiewicz, R.D., Abraham, R.T., Hoekstra, M.F., Aebersold, R., and Sonenberg, N. (1999). Regulation of 4E-BP1 phosphorylation: a novel two-step mechanism. Genes Dev. *13*, 1422–1437.

Graff, J.R., Konicek, B.W., Carter, J.H., and Marcusson, E.G. (2008). Targeting the eukaryotic translation initiation factor 4E for cancer therapy. Cancer Res. *68*, 631–634.

Han, D.W., Tapia, N., Hermann, A., Hemmer, K., Höing, S., Araúzo-Bravo, M.J., Zaehres, H., Wu, G., Frank, S., Moritz, S., et al. (2012). Direct reprogramming of fibroblasts into neural stem cells by defined factors. Cell Stem Cell *10*, 465–472.

Hanna, J., Markoulaki, S., Schorderet, P., Carey, B.W., Beard, C., Wernig, M., Creyghton, M.P., Steine, E.J., Cassady, J.P., Foreman, R., et al. (2008). Direct reprogramming of terminally differentiated mature B lymphocytes to pluripotency. Cell *133*, 250–264.

He, J., Kang, L., Wu, T., Zhang, J., Wang, H., Gao, H., Zhang, Y., Huang, B., Liu, W., Kou, Z., et al. (2012). An elaborate regulation of Mammalian target of rapamycin activity is required for somatic cell reprogramming induced by defined transcription factors. Stem Cells Dev. *21*, 2630–2641.

Hong, H., Takahashi, K., Ichisaka, T., Aoi, T., Kanagawa, O., Nakagawa, M., Okita, K., and Yamanaka, S. (2009). Suppression of induced pluripotent stem cell generation by the p53-p21 pathway. Nature *460*, 1132–1135.

Hou, P., Li, Y., Zhang, X., Liu, C., Guan, J., Li, H., Zhao, T., Ye, J., Yang, W., Liu, K., et al. (2013). Pluripotent stem cells induced from mouse somatic cells by small-molecule compounds. Science *341*, 651–654.

Hsieh, A.C., Liu, Y., Edlind, M.P., Ingolia, N.T., Janes, M.R., Sher, A., Shi, E.Y., Stumpf, C.R., Christensen, C., Bonham, M.J., et al. (2012). The translational landscape of mTOR signalling steers cancer initiation and metastasis. Nature *485*, 55–61.

Jackson, R.J., Hellen, C.U., and Pestova, T.V. (2010). The mechanism of eukaryotic translation initiation and principles of its regulation. Nat. Rev. Mol. Cell Biol. *11*, 113–127.

Jaenisch, R., and Young, R. (2008). Stem cells, the molecular circuitry of pluripotency and nuclear reprogramming. Cell *132*, 567–582.

Judson, R.L., Babiarz, J.E., Venere, M., and Blelloch, R. (2009). Embryonic stem cell-specific microRNAs promote induced pluripotency. Nat. Biotechnol. *27*, 459–461.

Kannan-Thulasiraman, P., Dolniak, B., Kaur, S., Sassano, A., Kalvakolanu, D.V., Hay, N., and Platanias, L.C. (2008). Role of the translational repressor 4E-BP1 in the regulation of p21(Waf1/Cip1) expression by retinoids. Biochem. Biophys. Res. Commun. *368*, 983–989.

Kawamura, T., Suzuki, J., Wang, Y.V., Menendez, S., Morera, L.B., Raya, A., Wahl, G.M., and Izpisúa Belmonte, J.C. (2009). Linking the p53 tumour suppressor pathway to somatic cell reprogramming. Nature *460*, 1140–1144.

Kim, K., Lerou, P., Yabuuchi, A., Lengerke, C., Ng, K., West, J., Kirby, A., Daly, M.J., and Daley, G.Q. (2007a). Histocompatible embryonic stem cells by parthenogenesis. Science *315*, 482–486.

Kim, K., Ng, K., Rugg-Gunn, P.J., Shieh, J.H., Kirak, O., Jaenisch, R., Wakayama, T., Moore, M.A., Pedersen, R.A., and Daley, G.Q. (2007b). Recombination signatures distinguish embryonic stem cells derived by parthenogenesis and somatic cell nuclear transfer. Cell Stem Cell *1*, 346–352.

Kim, D., Kim, C.H., Moon, J.I., Chung, Y.G., Chang, M.Y., Han, B.S., Ko, S., Yang, E., Cha, K.Y., Lanza, R., and Kim, K.S. (2009a). Generation of human induced pluripotent stem cells by direct delivery of reprogramming proteins. Cell Stem Cell *4*, 472–476.

Kim, J.B., Greber, B., Araúzo-Bravo, M.J., Meyer, J., Park, K.I., Zaehres, H., and Schöler, H.R. (2009b). Direct reprogramming of human neural stem cells by OCT4. Nature *461*, 649–3.

Kim, J.B., Sebastiano, V., Wu, G., Araúzo-Bravo, M.J., Sasse, P., Gentile, L., Ko, K., Ruau, D., Ehrich, M., van den Boom, D., et al. (2009c). Oct4-induced pluripotency in adult neural stem cells. Cell *136*, 411–419.

Kim, K., Doi, A., Wen, B., Ng, K., Zhao, R., Cahan, P., Kim, J., Aryee, M.J., Ji, H., Ehrlich, L.I., et al. (2010). Epigenetic memory in induced pluripotent stem cells. Nature *467*, 285–290.

Kim, J., Lengner, C.J., Kirak, O., Hanna, J., Cassady, J.P., Lodato, M.A., Wu, S., Faddah, D.A., Steine, E.J., Gao, Q., et al. (2011). Reprogramming of postnatal neurons into induced pluripotent stem cells by defined factors. Stem Cells *29*, 992–1000.

Koromilas, A.E., Lazaris-Karatzas, A., and Sonenberg, N. (1992). mRNAs containing extensive secondary structure in their 5' non-coding region translate efficiently in cells overexpressing initiation factor eIF-4E. EMBO J. *11*, 4153–4158.

Latham, K.E., Garrels, J.I., Chang, C., and Solter, D. (1991). Quantitative analysis of protein synthesis in mouse embryos. I. Extensive reprogramming at the one- and two-cell stages. Development *112*, 921–932.

Lu, R., Markowetz, F., Unwin, R.D., Leek, J.T., Airoldi, E.M., MacArthur, B.D., Lachmann, A., Rozov, R., Ma'ayan, A., Boyer, L.A., et al. (2009). Systems-level dynamic analyses of fate change in murine embryonic stem cells. Nature *462*, 358–362.

Marión, R.M., Strati, K., Li, H., Murga, M., Blanco, R., Ortega, S., Fernandez-Capetillo, O., Serrano, M., and Blasco, M.A. (2009). A p53-mediated DNA damage response limits reprogramming to ensure iPS cell genomic integrity. Nature *460*, 1149–1153.

Menendez, S., Camus, S., and Izpisua Belmonte, J.C. (2010). p53: guardian of reprogramming. Cell Cycle *9*, 3887–3891.

Okita, K., Nakagawa, M., Hyenjong, H., Ichisaka, T., and Yamanaka, S. (2008). Generation of mouse induced pluripotent stem cells without viral vectors. Science *322*, 949–953.

Pause, A., Belsham, G.J., Gingras, A.C., Donzé, O., Lin, T.A., Lawrence, J.C., Jr., and Sonenberg, N. (1994). Insulin-dependent stimulation of protein synthesis by phosphorylation of a regulator of 5'-cap function. Nature *371*, 762–767.

Petroulakis, E., Parsyan, A., Dowling, R.J., LeBacquer, O., Martineau, Y., Bidinosti, M., Larsson, O., Alain, T., Rong, L., Mamane, Y., et al. (2009). p53-dependent translational control of senescence and transformation via 4E-BPs. Cancer Cell *16*, 439–446.

Poulin, F., Gingras, A.C., Olsen, H., Chevalier, S., and Sonenberg, N. (1998). 4E-BP3, a new member of the eukaryotic initiation factor 4E-binding protein family. J. Biol. Chem. *273*, 14002–14007.

Rong, L., Livingstone, M., Sukarieh, R., Petroulakis, E., Gingras, A.C., Crosby, K., Smith, B., Polakiewicz, R.D., Pelletier, J., Ferraiuolo, M.A., and Sonenberg, N. (2008). Control of eIF4E cellular localization by eIF4E-binding proteins, 4E-BPs. RNA *14*, 1318–1327.

Rosenwald, I.B., Lazaris-Karatzas, A., Sonenberg, N., and Schmidt, E.V. (1993). Elevated levels of cyclin D1 protein in response to increased expression of eukaryotic initiation factor 4E. Mol. Cell. Biol. *13*, 7358–7363.

Sampath, P., Pritchard, D.K., Pabon, L., Reinecke, H., Schwartz, S.M., Morris, D.R., and Murry, C.E. (2008). A hierarchical network controls protein translation during murine embryonic stem cell self-renewal and differentiation. Cell Stem Cell 2, 448–460.

Schwanhäusser, B., Busse, D., Li, N., Dittmar, G., Schuchhardt, J., Wolf, J., Chen, W., and Selbach, M. (2011). Global quantification of mammalian gene expression control. Nature 473, 337–342.

Smith, Z.D., Nachman, I., Regev, A., and Meissner, A. (2010). Dynamic single-cell imaging of direct reprogramming reveals an early specifying event. Nat. Biotechnol. 28, 521–526.

Sonenberg, N., and Hinnebusch, A.G. (2009). Regulation of translation initiation in eukaryotes: mechanisms and biological targets. Cell 136, 731–745.

Stadtfeld, M., Maherali, N., Breault, D.T., and Hochedlinger, K. (2008). Defining molecular cornerstones during fibroblast to iPS cell reprogramming in mouse. Cell Stem Cell 2, 230–240.

Stoyanova, T., Cooper, A.R., Drake, J.M., Liu, X., Armstrong, A.J., Pienta, K.J., Zhang, H., Kohn, D.B., Huang, J., Witte, O.N., and Goldstein, A.S. (2013). Prostate cancer originating in basal cells progresses to adenocarcinoma propagated by luminal-like cells. Proc. Natl. Acad. Sci. USA 110, 20111–20116.

Subramanyam, D., Lamouille, S., Judson, R.L., Liu, J.Y., Bucay, N., Derynck, R., and Blelloch, R. (2011). Multiple targets of miR-302 and miR-372 promote reprogramming of human fibroblasts to induced pluripotent stem cells. Nat. Biotechnol. 29, 443–448.

Takahashi, K., and Yamanaka, S. (2006). Induction of pluripotent stem cells from mouse embryonic and adult fibroblast cultures by defined factors. Cell 126, 663–676.

Tanabe, K., Nakamura, M., Narita, M., Takahashi, K., and Yamanaka, S. (2013). Maturation, not initiation, is the major roadblock during reprogramming toward pluripotency from human fibroblasts. Proc. Natl. Acad. Sci. USA 110, 12172–12179.

Thoreen, C.C., Chantranupong, L., Keys, H.R., Wang, T., Gray, N.S., and Sabatini, D.M. (2012). A unifying model for mTORC1-mediated regulation of mRNA translation. Nature 485, 109–113.

Utikal, J., Polo, J.M., Stadtfeld, M., Maherali, N., Kulalert, W., Walsh, R.M., Khalil, A., Rheinwald, J.G., and Hochedlinger, K. (2009). Immortalization eliminates a roadblock during cellular reprogramming into iPS cells. Nature 460, 1145–1148.

Warner, J.R., Knopf, P.M., and Rich, A. (1963). A multiple ribosomal structure in protein synthesis. Proc. Natl. Acad. Sci. USA 49, 122–129.

Warren, L., Manos, P.D., Ahfeldt, T., Loh, Y.H., Li, H., Lau, F., Ebina, W., Mandal, P.K., Smith, Z.D., Meissner, A., et al. (2010). Highly efficient reprogramming to pluripotency and directed differentiation of human cells with synthetic modified mRNA. Cell Stem Cell 7, 618–630.

Yu, J., Vodyanik, M.A., Smuga-Otto, K., Antosiewicz-Bourget, J., Frane, J.L., Tian, S., Nie, J., Jonsdottir, G.A., Ruotti, V., Stewart, R., et al. (2007). Induced pluripotent stem cell lines derived from human somatic cells. Science 318, 1917–1920.

Zhou, H., Wu, S., Joo, J.Y., Zhu, S., Han, D.W., Lin, T., Trauger, S., Bien, G., Yao, S., Zhu, Y., et al. (2009). Generation of induced pluripotent stem cells using recombinant proteins. Cell Stem Cell 4, 381–384.

Zoncu, R., Efeyan, A., and Sabatini, D.M. (2011). mTOR: from growth signal integration to cancer, diabetes and ageing. Nat. Rev. Mol. Cell Biol. 12, 21–35.